To appear in The Astrophysical Journal Letters
Preprint typeset using LaTeX style emulateapj v. 04/03/99

FAR-UV EMISSION FROM ELLIPTICAL GALAXIES AT $Z = 0.55$[1]

Thomas M. Brown[2], Charles W. Bowers, Randy A. Kimble
Laboratory for Astronomy & Solar Physics, Code 681, NASA/GSFC, Greenbelt, MD 20771.
tbrown@pulsar.gsfc.nasa.gov, bowers@band2.gsfc.nasa.gov, kimble@ccd.gsfc.nasa.gov.
Henry C. Ferguson
Space Telescope Science Institute, 3700 San Martin Drive, Baltimore, MD 21218. ferguson@stsci.edu.

To appear in The Astrophysical Journal Letters

ABSTRACT

The restframe UV-to-optical flux ratio, characterizing the "UV upturn" phenomenon, is potentially the most sensitive tracer of age in elliptical galaxies; models predict that it may change by orders of magnitude over the course of a few Gyr. In order to trace the evolution of the UV upturn as a function of redshift, we have used the far-UV camera on the Space Telescope Imaging Spectrograph to image the galaxy cluster CL0016+16 at $z = 0.55$. Our $25'' \times 25''$ field includes four bright elliptical galaxies, spectroscopically confirmed to be passively evolving cluster members. The weak UV emission from the galaxies in our image demonstrates that the UV upturn is weaker at a lookback time $\sim$5.6 Gyr earlier than our own, as compared to measurements of the UV upturn in cluster E and S0 galaxies at $z = 0$ and $z = 0.375$. These images are the first with sufficient depth to demonstrate the fading of the UV upturn expected at moderate redshifts. We discuss these observations and the implications for the formation history of galaxies.

Subject headings: galaxies: evolution — galaxies: stellar content — ultraviolet: galaxies

1. INTRODUCTION

Because they are composed of old, passively evolving populations, elliptical galaxies offer great promise for tracing the evolution of the Universe. Whether elliptical galaxies formed through hierarchical merging or monolithic collapse, one of the major goals in extragalactic studies is the determination of the "redshift of formation," z_F, that marks the age where most of the stars in early-type galaxies formed. Recent studies of galaxy clusters out to $z \sim 1$ indicate that most of the star formation had to be completed at high redshift ($z \gtrsim 3$), followed by quiescent evolution thereafter (Stanford, Eisenhardt, & Dickinson 1998; Kodama et al. 1998).

The UV upturn is a sharp rise in the spectra of E and S0 galaxies shortward of restframe 2500 Å. It provides a sensitive tracer of age for the oldest stars in these galaxies, and can potentially constrain z_F. Traditionally characterized by the $1550 - V$ color, the UV upturn in local galaxies originates in a population of hot horizontal branch (HB) stars and their UV-bright progeny (see Brown et al. 2000 and references therein). As first noted by Greggio & Renzini (1990), the UV upturn should evolve rapidly with age, through the evolution of HB morphology and the main sequence turnoff mass. Although all models of elliptical galaxy evolution predict a rapid evolution in the UV upturn (e.g., Tantalo et al. 1996), the timing for the UV upturn onset depends strongly upon model parameters.

We have been undertaking a series of observations to trace the evolution of the UV upturn as a function of redshift. Faint Object Camera (FOC) observations of Abell 370 ($z = 0.375$) provided the first detection of far-UV emission from quiescent elliptical galaxies above $z = 0.05$ (Brown et al. 1998). The very strong UV emission found at $z = 0.375$ suggests no evolution in the UV upturn between our own epoch and one 4 Gyr earlier, a finding inconsistent with some models of galaxy evolution, and apparently consistent only for high values of z_F. Here, we describe observations that trace the UV upturn to higher redshift. We used the far-UV camera on the Space Telescope Imaging Spectrograph (STIS) to measure the UV emission from four giant elliptical galaxies in the cluster CL0016+16 at $z = 0.55$. Ground-based spectroscopy confirms their passive evolution and cluster membership (Dressler & Gunn 1992); morphological classification comes from Wide Field Planetary Camera 2 (WFPC2) imaging in the F555W and F814W bands (Smail et al. 1997). We assume the currently popular cosmology of $\Omega_M = 0.3$, $\Omega_\Lambda = 0.7$, and $H_o = 67$ km s^{-1} Mpc^{-1}, although our results are more sensitive to z_F than to the assumed cosmology.

2. OBSERVATIONS

Using the STIS far-UV camera on 19 Aug and 21 Aug 1999, we observed a $25'' \times 25''$ field centered at RA(J2000)=$0^h18^m33.2^s$ and Dec(J2000)=$16^o26'9.7''$ in the cluster CL0016+16. The total exposure was 27892 sec; 10 frames were taken in two visits, with dithering by 6 pixels to smooth out small-scale detector variations. We used the crystal quartz filter (F25QTZ) for a bandpass that spans 1450–2000 Å, thus reducing the sky background from geocoronal O I and Lyman-α to negligible levels at little cost in galaxy light, as the redshift ($z = 0.55$) puts the Lyman limit at the short wavelength cutoff. Because the long wavelength cutoff of this bandpass is due to detector sensitivity, red leak is also negligible; we avoid the problematic red leak and red grating scatter that hampered earlier attempts to measure the UV upturn at moderate redshift (e.g., Windhorst et al. 1994). The photometric calibration is reliable at the 0.15 mag level (Baum et al. 1998). Recent efforts have revised the calibration slightly; we assume the latest revision, with an accuracy that should be better than 0.15 mag. For reference, we assume that a flat spectrum of 1.036×10^{-16} erg

[1]Based on observations with the NASA/ESA Hubble Space Telescope obtained at the Space Telescope Science Institute, which is operated by AURA, Inc., under NASA contract NAS 5-26555.

[2] NOAO Research Associate.

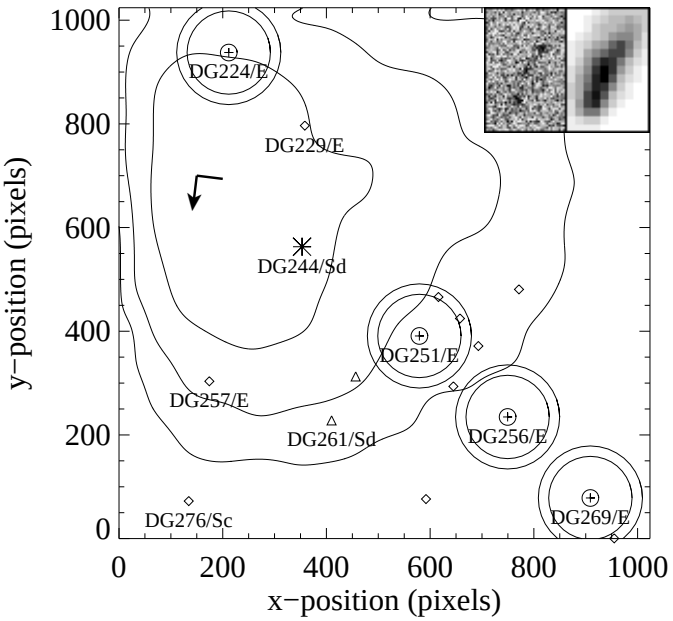

FIG. 1– A schematic of the STIS image. Each bright cluster E galaxy is denoted by a cross, photometric aperture, and sky annulus. When there is a strong dark background, its shape follows the contours shown (contour levels are at 2×, 5×, and 10× the lowest dark rate). A non-cluster spiral (asterisk) was used for astrometry and registration; it is shown in the inset at 4× magnification, as it appears in the STIS (left) and WFPC2 (right) images. Triangles denote $\sim 8\sigma$ detections, and diamonds mark other objects from the Smail et al. (1997) catalog at $I_{814} < 24$ mag. Galaxies appearing in the Dressler & Gunn (1992) catalog are labeled, along with their morphology (Smail et al. 1997).

sec^{-1} cm^{-2} Å^{-1} produces one count per sec in the STIS bandpass. A full description of the instrument can be found in Woodgate et al. (1998) and Kimble et al. (1998).

Unfortunately, the mean temperature of the far-UV camera has increased since STIS commissioning, and the dark background increases as a function of temperature. This increase appears as a "glow" that is strongest in the upper left-hand quadrant of the detector (Figure 1), where the dark rate can be 20 times higher than the nominal 6×10^{-6} cts sec^{-1} pix^{-1}. The glow varies from weak to strong in our 10 frames.

The Galactic foreground extinction toward our field was thought to be $E(B-V) = 0.022$ mag at the time these observations were planned, based upon H I maps (Burstein & Heiles 1984). The subsequent release of a new extinction map (Schlegel, Finkbeiner, & Davis 1998), based upon an IRAS map of the Galactic dust, revises the extinction estimate to 0.057 mag. The increased dark background and higher extinction both work to decrease the sensitivity of our observations to far-UV emission, but do not preclude constraints on the UV upturn. When accounting for this extinction, we assume the empirical model of Cardelli, Clayton, & Mathis (1989), which has been parameterized and tested from the UV to IR.

Our STIS field includes four giant E galaxies (see Figure 1); three are detected at $>2.5\sigma$ significance. We detect three other objects from the Smail et al. (1997) catalog at a significance of $\sim 8\sigma$. We use the bright background spiral, DG244 ($z = 0.6577$; Dressler & Gunn 1992), to confirm the registration of our frames, and to determine the positions of the fainter galaxies. The accuracy of relative astrometry within WFPC2 or STIS images is better than $0.1''$, but the accuracy of absolute astrometry can be worse than $1''$, so the positions of objects in the STIS field are determined relative to this bright spiral. Most of the objects in our chosen field are too red and faint to be detected by STIS; their non-detection does not suggest an unexpected lack of sensitivity, and all detected and non-detected objects are consistent with the expected range of spectral energy distributions (SEDs). STIS repeatedly images UV-bright stars (e.g., globular cluster NGC6681), and no drop in sensitivity is apparent in observations before and after our observation of the cluster CL0016+16.

3. DATA REDUCTION

The STIS data was reduced via methods nearly identical to those used for the Hubble Deep Field South, to which we refer the interested reader for more details (Gardner et al. 1999). In brief, the images were processed via the standard pipeline, excluding the dark subtraction, low-frequency flat field correction, and geometric correction. Dark frames from July through August of 1999 were processed in the same manner, and those with a strong glow ($> 2\times10^{-5}$ cts sec^{-1} pix^{-1}) were summed and fit with a cubic spline to produce a profile appropriate for our CL0016+16 observations (the shape of the glow changes slowly with time, and so recent darks are required for this fit). A flat component and glow component to the dark background were then subtracted from each CL0016+16 frame, and then the flat field correction was applied. The frames were registered by integer shifts and summed via the DRIZZLE package. The pixels in each frame were weighted by the ratio of the exposure time squared to the dark count variance, including a hot pixel mask. The algorithm weights the exposures by the square of the signal-to-noise (S/N) ratio for sources that are fainter than the background, thus optimizing the summation to account for the temporal and spatial variations in the dark background. The statistical errors in the final drizzled image (cts pix^{-1}), for objects below the background, are given by the square root of the final drizzled weights map scaled by the exposure time. Geometric correction, which tends to smear out the pixels through non-integer shifts, was not applied. For small dithers and large extraction apertures, it is not needed for object registration.

WFPC2 F814W data for the same field were obtained from the STScI archive and reduced via standard techniques, including cosmic-ray rejection and masking of problematic pixels. The total exposure in the F814W image is 16800 sec. The summed image was used to determine the restframe optical-band flux for each elliptical galaxy, and to determine the relative positions of objects in the STIS field.

4. PHOTOMETRY

We performed aperture photometry on the far-UV frames using IDL, taking a weighted average of the flux within a 16-pixel ($0.4''$) radius, and a weighted average of the flux within a sky annulus of radii 80 and 100 pixels. The aperture includes the bright core of each galaxy, as they appear in the WFPC2 data. The aperture is small enough to minimize the background in the far-UV measurement, but large enough to avoid significant errors in the expected encircled energy (due to the uncertainty in the position of the galaxies); it is also relevant to measurements made of local galaxies, which use a nuclear aperture (see §5). The weighting used the map of statistical errors (see §3), in the sense that pixels were weighted less if they had less exposure (due to masked pixels) or higher dark count rates. This weighting did *not* weigh by counts in the *data* frame, which would obviously bias the photometry toward pixels with more source

TABLE 1: Photometry

	position		catalog				aperture phot.		restframe	$1550-V$
	x (pix)	y (pix)	Smail[a] ID	DG[b] ID	Morph. type[a]	z[b]	FUVQTZ (cts)	F814W (DN)	$1550-V$ (mag)	3σ limit (mag)
	212	938	650	224	E/S0	0.5382	33± 29	20577±94	$3.7^{+2.3}_{-0.7}$	2.3
Cluster	579	391	724	251	E	0.5433	61± 22	34388±126	$3.6^{+0.5}_{-0.3}$	2.8
Elliptical	749	234	725	256	E	0.5324	40± 15	30450±111	$4.0^{+0.5}_{-0.3}$	3.1
Galaxies	909	78	745	269	E	0.5405	40± 15	28964±79	$3.9^{+0.5}_{-0.3}$	3.1
	Sum of four cluster elliptical galaxies						174±43	114379±204	$3.8^{+0.3}_{-0.2}$	3.2
Other	353	563	677	244	Sd	0.6582	280± 32	14693±67	N/A	N/A
Detected	410	228	705	261	Sd	...	177± 22	3831±69	N/A	N/A
Galaxies	456	313	696	...	?	...	185± 24	858±83	N/A	N/A

[a] Smail et al. (1997).
[b] Dressler & Gunn (1992).

counts. We determined the local sky value from the mean instead of the median in the sky annulus, because most pixels are ones and zeros. Note that alternate methods for determining the sky background (e.g., fitting a surface to the local residual background) yield results well within the 1σ photometric errors. The positions of objects in the STIS image were determined from the geometrically-corrected WFPC2 F814W frame, relative to the spiral galaxy DG244 (see Figure 1). Calculation of position in the STIS frame involves a rescaling, rotation, translation, and geometric distortion, using the geometric distortion coefficients of Malumuth (1997). We tested our positioning algorithm using WFPC2 and STIS images of the globular cluster NGC6681, which was observed with STIS numerous times before and after our CL0016+16 observations at various roll angles and positions. Absolute positional accuracy for objects in the STIS frame is 1–2 STIS pixels, well within the 16-pixel radius used for aperture photometry.

For the WFPC2 F814W frames, we performed aperture photometry with the IRAF package PHOT, using a 4-pixel radius ($0.4''$), and a sky annulus of radii 20 and 25 pixels, thus matching the photometry done in the STIS image. Note that this aperture size would produce encircled energy agreement at the 5% level for point sources, and better agreement for extended sources (Robinson 1997; Holtzman et al. 1995), so the uncertainty in encircled energy contributes less than 0.1 mag to $1550-V$. We do not perform an aperture correction because we are only interested in colors, not the absolute fluxes.

Photometry was performed on all objects with $I_{814} < 24$ mag in the Smail et al. (1997) catalog, plus a faint object (#696) that is obvious in the STIS image but faint in the WFPC2 frames. Table 1 gives the photometry for the four giant elliptical galaxies, plus three objects detected at $\sim 8\sigma$ in the STIS image.

5. INTERPRETATION

The UV upturn is traditionally characterized by the restframe $1550-V$ color (see Burstein et al. 1988). Conversion to restframe $1550-V$ from our observed bandpasses depends upon the assumption of an SED. Brown et al. (1998) used the spectra of three local elliptical galaxies (NGC1399, M60, and M49) to convert their observed FOC bandpasses to restframe $1550-V$, and we used the same spectra here. We redshifted the spectra of NGC1399, M60, and M49 to $z = 0.55$, and then applied a foreground reddening of $E(B-V) = 0.057$ mag (Schlegel et al. 1998). We then used the IRAF CALCPHOT routine to calculate the STIS and WFPC2 countrates, giving:

$$1550-V = -2.5 \times \log_{10}(cps_{FUV}/dps_{F814W}) - 3.8 \text{ mag},$$

where cps_{FUV} is the STIS countrate (cts sec^{-1}), and dps_{F814W} is the WFPC2 countrate (DN sec^{-1}). This conversion gives the restframe $1550-V$ values shown in Table 1. We also calculate the $1550-V$ assuming the 3σ upper limit to the far-UV flux. Note that the $1550-V$ values in Table 1 would be redder if the foreground extinction is closer to $E(B-V) = 0.022$ mag (see §2), or if the far-UV SEDs are dominated by post-AGB stars (see below). The $1550-V$ color for the sum of the giant elliptical galaxy photometry gives an average measurement of the UV upturn in our sample.

Although we are looking to a significantly earlier epoch, the assumption of a model SED over an empirical SED makes little difference for the restframe V, because the observed F814W band overlaps with restframe V. For example, assuming that E galaxies are $\sim$5 Gyr old at $z = 0.55$, we calculated the $\mathrm{F814W}_{observed} - V_{rest\,frame}$ color using the Bruzual & Charlot (1993) instantaneous burst SED of age 5 Gyr, and the NGC1399 SED, assuming $z = 0.55$ with a foreground reddening of $E(B-V) = 0.057$. The difference in $\mathrm{F814W}_{observed} - V_{rest\,frame}$ for the two SEDs was only 0.02 mag. The assumed SED has somewhat more effect on the far-UV. Our STIS bandpass spans restframe 935–1290 Å, and the $1550-V$ color is based on the average flux from 1250–1850 Å. However, we note that no model SED has been tested in the far-UV for passively-evolving galaxies at moderate redshift, and thus we prefer empirical SEDs. Younger galaxies should have a larger contribution from relatively hot post-AGB stars, instead of HB stars (see Brown et al. 1997), so our conversion might systematically produce a bluer $1550-V$ than the true restframe $1550-V$. Alternatively, if younger galaxies are dominated by even cooler HB stars than those in local galaxies, we are calculating a redder $1550-V$ than the true value.

Another source of systematic error is the aperture size. Local E galaxies have been measured through $14''$ diameter aperture (1.5 kpc at the distance of Virgo), sampling only the nuclear flux (Burstein et al. 1988). The $z = 0.375$ measurements were made through a $1.82''$ diameter aperture (9.8 kpc at the distance of Abell 370), including all of the galactic light detected by the FOC (Brown et al. 1998). We have measured the flux from our $z = 0.55$ galaxies through a $0.8''$ diameter aperture (5.4 kpc at the distance of CL0016+16), enclosing the light from the galaxy cores. Our aperture is 3.6 times larger than that used for local galaxies, but 1.8 times smaller than that used for the Abell 370 galaxies. Ohl et al. (1998) found that local E galaxies usually (but not always) become redder in $1550-V$ at increasing radius; the color gradient is not large (0.1–0.5 mag) over radii 7–$25''$, and the color of the integrated light in an in-

creasing aperture will change even less, because most of the light comes from the central ~ 2 kpc even in our larger apertures. Thus, the aperture effects should be small, but perhaps non-negligible (~ 0.1 mag).

6. DISCUSSION

The average restframe $1550-V$ color for the four giant E galaxies at $z = 0.55$ is much redder than that observed in clusters at $z = 0$ and $z = 0.375$. At the 3σ upper limit to the far-UV flux, none of the $z = 0.55$ galaxies are as blue as the strong UV-upturn galaxies observed locally (e.g., M60 or NGC1399). Ideally, one would want to compare galaxies at similar velocity dispersion (σ_v) in each epoch, because σ_v can be measured in a model-independent manner, and because the UV upturn strongly correlates with σ_v locally (Burstein et al. 1988). Measurements of σ_v are unavailable for some of the $z = 0.375$ galaxies and all of the $z = 0.55$ galaxies, but these galaxies were selected from the brightest and largest in each cluster, and would likely show strong UV upturns if observed locally. The faint far-UV emission from the $z = 0.55$ galaxies thus demonstrates that the UV upturn is sensitive to age. We plot these UV upturn measurements in Figure 2, along with the models of Tantalo et al. (1996), which trace the chemical evolution of elliptical galaxies under the assumption of gas infall. Note that the scatter in local UV upturn measurements is affected by the wide range of sizes and luminosities in the sample; the moderate-redshift samples are more homogeneous, but the measurements themselves are less statistically significant.

In the Tantalo et al. (1996) models, the UV upturn appears at an age of ~ 6.5 Gyr, becomes quite blue by 9 Gyr, and is flat thereafter. Assuming the models are correct and that the oldest stars in cluster E galaxies all formed at a common redshift, our measurements imply $z_F \sim 4$. If elliptical galaxies form through hierarchical merging, the age of the oldest stars may predate such merging; alternatively, the age of the oldest stars may reflect the age of the galaxies themselves, if they were assembled through monolithic collapse. However, the Tantalo et al. (1996) models rely on several parameters (e.g., time of onset for galactic winds, efficiency of the star formation rate, accretion timescale, etc.) that can be tuned to delay or accelerate the onset of the UV upturn. In this sense, our results say more about the evolution of HB morphology than z_F; if galaxies form their oldest stars at $z > 4$, our data imply that a blue HB population cannot arise until ages greater than 7 Gyr.

Although the elliptical galaxies in our program are chosen through ground-based spectroscopy that confirms their passive evolution, the strong UV upturn found at $z = 0.375$ could theoretically be due to residual star formation instead of evolved populations. This star formation would have to cease by the present epoch, because the UV emission from local cluster elliptical galaxies is clearly due to HB stars instead of star formation. If all clusters are alike, our new $z = 0.55$ observations reinforce the case against star formation at $z = 0.375$, because such star formation would likely be even stronger at a larger lookback time. Measurements at $z = 0$, 0.375, and 0.55 demonstrate that the UV upturn rises sharply over a few Gyr, and then levels off. This line of inquiry into the evolution of galaxies is still in the early stages, and further observations are needed over a range of redshifts. Such measurements should become much more feasible in HST Cycle 10, once a cooler is connected to STIS (reducing the dark background to minimal levels).

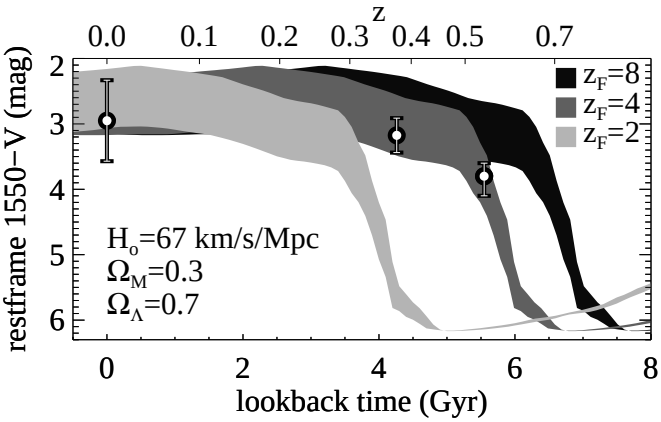

FIG. 2– Evolution of the restframe $1550-V$ color according to the models of Tantalo et al. (1996) (shaded), viewed as a function of lookback time, assuming a reasonable set of cosmological parameters and three different epochs of galaxy formation (labeled). The spread in $1550-V$ is bounded by models at $M = 3\times10^{12}$ and $M = 10^{12}M_\odot$. Note the sudden onset of UV emission caused by the appearance of metal-rich hot HB stars. The points represent the mean $1550-V$ color measured for quiescent E and S0 galaxies in clusters at $z = 0$ (Virgo, Fornax, and Coma; Burstein et al. 1988), $z = 0.375$ (Abell 370; Brown et al. 1998), and $z = 0.55$ (CL0016+16). The error bars at $z = 0$ and $z = 0.375$ give the rms in galaxy colors (photometric errors are negligible); the error bar at $z = 0.55$ gives the photometric error for the summed galaxies (rms in the galaxy colors is smaller).

Support for this work was provided by NASA through the STIS GTO team funding. TMB acknowledges support at GSFC by NAS 5-6499D. We wish to thank the MORPHS project for making their cluster data and catalogs publicly available.

REFERENCES

Baum, S., et al. 1998, Space Telescope Imaging Spectrograph Instrument Handbook, (Baltimore: STScI), 315
Brown, T. M., Bowers, C. W., Kimble, R. A., Sweigart, A. V., & Ferguson, H. C. 2000, ApJ, 531, in press, astro-ph/9909391
Brown, T.M., Ferguson, H.C., Davidsen, A.F., & Dorman, B. 1997, ApJ, 482, 685
Brown, T. M., Ferguson, H. C., Deharveng, J.-M., & Jedrzejewski, R. I. 1998, ApJ, 508, L139
Bruzual, G., & Charlot, S. 1993, ApJ, 405, 538
Burstein, D., Bertola, F., Buson, L. M., Faber, S. M., & Lauer, T. R. 1988, ApJ, 328, 440
Burstein, D., & Heiles, C. 1984, AJ, 87, 1165
Cardelli, J. A., Clayton, G. C., & Mathis, J. S. 1989, 345, 245
Dressler, A., & Gunn, J. E. 1992, ApJS, 78, 1
Gardner, J. P., et al. 1999, AJ, in press
Greggio, L., & Renzini, A. 1990, ApJ, 364, 35
Holtzman, J., et al. 1995, PASP, 107, 156
Kimble, R. A., et al. 1998, ApJ, 492, L83
Kodama, T., Arimoto, N., Barger, A. J., & Aragón-Salamanca, A. 1998, A&A, 334, 99
Malumuth, E. 1997, in "STIS FUV-MAMA Geometric Distortion," http://hires.gsfc.nasa.gov
Ohl, R. G., et al. 1998, ApJ, 505, L110
Robinson, R. 1997, in "Examining the STIS Point Spread Function," http://hires.gsfc.nasa.gov
Schlegel, D. J., Finkbeiner, D. P., & Davis, M. 1998, ApJ, 500, 525
Smail, I., Dressler, A., Couch, W. J., Ellis, R. S., Oemler, A., Jr., Butcher, H., & Sharples, R. M. 1997, ApJS, 110, 213
Stanford, S. A., Eisenhardt, P. R., & Dickinson, M. 1998, ApJ, 492, 461
Tantalo, R., Chiosi, C., Bressan, A., & Fagotto, F. 1996, A&A, 311, 361
Windhorst, R. A., et al. 1994, in Frontiers of Space and Ground-Based Astronomy, ed. W. Wamsteker et al. (Dordrecht: Kluwer), 663
Woodgate, B. E., et al. 1998, PASP, 110, 1183